J. Fluid Mech. (1988), *vol.* 195, *pp.* 437–462
Printed in Great Britain

The resolution of shocks and the effects of compressible sediments in transient settling

By F. M. AUZERAIS, R. JACKSON AND W. B. RUSSEL
Department of Chemical Engineering, Princeton University, Princeton, NJ 08544, USA

(Received 3 February 1987 and in revised form 17 March 1988)

The consolidation or concentration of suspended particulate solids under the influence of gravitational forces is a problem of widespread practical and theoretical interest. The literature, which is scattered over several fields, contains most of the elements necessary for a complete understanding of gravity settling, but considerable controversy and confusion persists about their synthesis. Here we propose to construct a quantitative theory covering the full range of processes from transient settling of large, stable particles to the slow consolidation of flocculated suspensions of submicron particles. Conditions for the existence of shocks are identified and the basic equations describing the phenomena are solved numerically for several Péclet numbers.

1. Introduction

The operations of gravity settling and filtration of dispersions of micron and submicron particles in liquids are fundamental to a wide variety of natural and industrial processes. Several classical papers provide considerable physical insight into the phenomena and the essential features of the mathematical formulation. Coe & Clevenger (1916) defined the basic physics for continuous thickeners, while Kynch (1952) formulated the mathematical treatment of batch settling, both focusing on concentration profiles in the settling phase. Meanwhile, Terzaghi (1925), concerned with soil mechanics, postulated a model for the consolidation of sediments.

Since its original publication a good deal of controversy has gathered about the Kynch analysis. This is concerned with the selection of the physically correct results in cases with more than one formal solution of the mathematical problem. The question centres on conditions which must be satisfied at a discontinuity in concentration, e.g. at the surface of the settled sediment or within the suspension between a region of varying concentration and the uniform region above it. Dixon (1977) pointed out that inertial effects, which are justifiably neglected for small particles in regions where the concentration varies continuously, can never be neglected across a true discontinuity. There the jump in momentum flux which accompanies the jump in concentration must be balanced by a corresponding jump in stress transmitted through the particle phase. Consequently, Dixon concluded that a shock can never separate two regions of free settling, making some of the solutions identified by Kynch inadmissible. But this conclusion leaves a whole range of systems and initial conditions for which, apparently, no consistent solution can be found.

Another aspect of the theory, namely Kynch's assumption that the settled sediment at the bottom of the vessel is incompressible, is clearly unrealistic for flocculated systems which are compacted under gravity as the depth of the sediment

increases. Though the stresses involved here are much smaller, the situation is analogous mathematically to the drained consolidation of soils, originally treated by Terzaghi (1925). Michaels & Bolger (1962) addressed flocculated suspensions and assumed that compaction takes place under the combined influence of gravity, fluid-particle drag forces, and stresses transmitted through the particle phase, with both the transmitted stress and the resistance to fluid flow in the sediment depending only on the solids concentration. Shirato *et al.* (1970) obtained numerical solutions for a similar model, and these were tested against experimental measurements by the above authors, Shin & Dick (1974), and Kos & Adrian (1974). Adorján (1975) developed a theory of sediment compression, based on the equilibrium of compressive, viscous and gravitational forces. Buscall & White (1987) studied the compaction of structured sediments because of their common occurrence in chemical processes. Fitch (1983) treated the compression of sediments in steady state thickening, and Tiller (1981) attacked the difficult problem of coupling the Kynch theory for the free settling region with a solution for the compacting sediment. Problems arose, however, because of the nonlinearity of the governing equations, which generates multiple solutions and hence discontinuities. Controversy has persisted in the identification of the allowable discontinuities in the settling phase and the coupling of the solution for this phase with a compressible sediment.

Our treatment starts with the complete equations of motion for the fluid–particle system, including all the forces active in both the settling and sediment phases, i.e. gravity, inertia, and viscous and interparticle stresses. Proper scaling of the equations then relates the appearance of large gradients in concentration to particular dimensionless groups, and permits the construction of 'inner solutions' in these regions of rapid variation, which can be matched to 'outer solutions' in the regions of slow variation to yield the jump conditions across the shocks without *ad hoc* assumptions. The analysis, therefore, predicts unambiguously concentration profiles from the bottom of the sediment to the clear fluid above the settling phase for both stable and flocculated suspensions. It is important to note that effects such as short-circuiting and channelling are not considered.

2. The theory of hindered settling

In 1916 Coe & Clevenger published a now classical account of the settling of metallurgical slimes. Their clear account of the settling process recognized that the colloidal particles quite rapidly aggregate into flocs, which subsequently separate from the liquid by gravity settling. For batch settling they identified four zones, an upper layer of clear liquid separated from the suspension by a sharp interface, a layer of flocculated suspension of uniform density settling at a uniform rate, a layer within which the density increases continuously with depth and, finally, a layer containing flocs in contact supported by forces transmitted through the contact points. In the upper layer they envisaged the flocs to move essentially under the influence of gravity and hydrodynamic drag forces only, though they recognized, from the peculiarly interlocking structure of flocculated pulp, that there are points of contact between the flocs even in these zones. Two types of settling behaviour were distinguished: type 1, in which the thickness of the third zone is very small, and type 2, in which it is a significant fraction of the total depth of the suspension. Coe & Clevenger's work provided a basis for the design of continuous thickeners from batch settling tests.

Kynch (1952) was apparently the first to formulate a mathematical treatment of

the details of batch settling. He was concerned only with a suspension of identical particles moving under the influence of gravity and hydrodynamic drag forces in balance. Then for given particles and suspending fluid, the sedimentation velocity, or equivalently the downward flux of particles, is a function only of ϕ, the volume fraction of solid material, and as the particle concentration increases the velocity decreases. Using the method of characteristics, Kynch found that, in certain circumstances, complete solutions could be found only if the possibility of discontinuities, or shocks, was admitted.

2.1. *Kynch theory*

The behaviour of the freely settling suspension is governed by the conservation equation for the particles,

$$\frac{\partial \phi}{\partial t} + \frac{\partial [\phi U(\phi)]}{\partial x} = 0, \tag{1}$$

where $U(\phi)$ denotes the sedimentation velocity with x positive measuring downward from an origin at the top of the liquid ($x = 0$). Equation (1) may be written as

$$\frac{\partial \phi}{\partial t} + \frac{\mathrm{d}[\phi U(\phi)]}{\mathrm{d}\phi} \frac{\partial \phi}{\partial x} = 0, \tag{2}$$

which is a partial differential equation whose properties are determined by the form of the sedimentation curve $\phi U(\phi)$ *vs.* ϕ.

The characteristics of (2) are contours of constant ϕ with slopes given by

$$\frac{\mathrm{d}x}{\mathrm{d}t} = -\frac{\mathrm{d}[\phi U(\phi)]}{\mathrm{d}\phi}, \tag{3}$$

so they are straight lines in the (x, t)-plane. Clear fluid above the sedimenting suspension is separated from the suspension by a sharp interface, while below a layer of particles rest in contact with each other and with the bottom of the vessel. This layer is regarded as incompressible, with its bulk density fixed at ϕ_{m}. In these circumstances the velocities of the interfaces separating the suspension from the clear fluid above and the settled material below are determined by continuity. These solutions highlight the importance of the concentration dependence of the volume flux $\phi U(\phi)$.

Despite the apparent simplicity of the case treated by Kynch, a variety of behaviour is possible depending on the shape of the flux curve and the initial spatial distribution of the particles. For the usual shape of this curve, plotted in figure 1, Rhee, Aris & Amundson (1986) illustrate the method of characteristics by considering different uniform initial concentrations and identify three essentially different types of behaviour. In the first a zone of constant concentration falls with constant speed to meet with the rising sediment. In the second a zone of continuously varying concentration separates the settled material below from a uniform suspension above; consequently the speed of descent of this zone decreases before settling is complete. The third resembles the second, except that a discontinuity in concentration develops between the region of varying concentration and the uniform region above. The distinction between the first type of behaviour and the other two is analogous to Coe & Clevenger's distinction between two types of settling. Other cases can be found in the literature (Wallis 1963; McRoberts & Nixon 1976).

The solution is complete and single-valued when the characteristics springing from

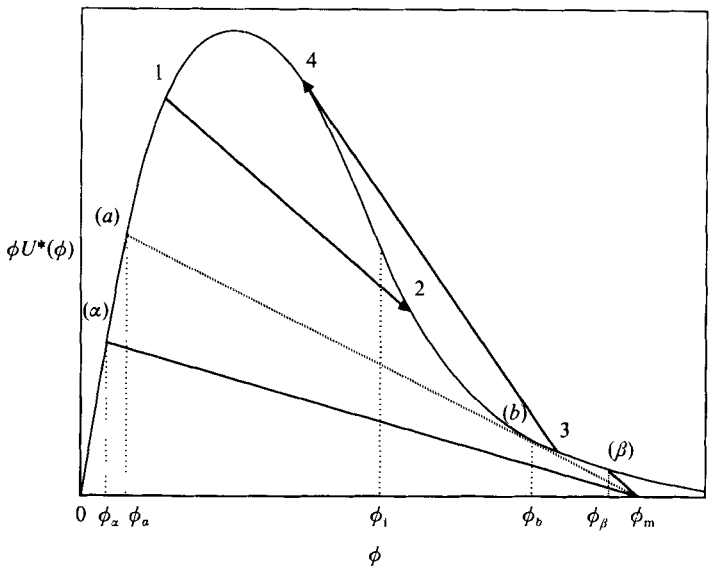

FIGURE 1. Schematic illustration of a flux curve with associated discontinuities.

the $t = 0$ axis fill the entire (x,t)-plane above the settled sediment without intersecting. Often, however, characteristics intersect, indicating an unacceptable multiplicity of solutions. This is resolved by introducing a discontinuity separating regions in which the solution varies continuously.

A satisfactory theory of settling suspensions with compressible sediments, including the identification of regions of rapidly varying concentration forming 'shocks', must recognize the transmission of stresses between the particles. In a settling region where the concentration of particles varies smoothly these would have negligible influence. However, they generate a resultant force which depends on the concentration gradient and is therefore non-negligible in regions of very rapidly varying concentration, even when the concentration itself is not very large. At higher concentrations they become larger and balance the gravitational forces, thereby supporting the sediment. They therefore play an important role in the mechanical structure of 'shocks', making it possible to model in detail the mechanics of the transition between the settling zone and the sediment surface, thus eliminating the need for *ad hoc* assumptions regarding the characteristics of the Kynch equation there.

2.2. *The momentum equation*

In order to introduce the forces omitted in arriving at the flux expression used in the continuity equation (1), we must consider momentum balances for the liquid–solid system, including both inertia and stresses transmitted through the sediment, as advocated by Dixon (1977).

Definitive forms for the momentum balances, valid over the whole range of particle sizes, concentrations and densities, are not available. All existing attempts to formulate these involve *ad hoc* assumptions, some of which are controversial. Fortunately, for the present purpose, the controversial aspects of such equations are not important. The results of importance (inequalities (24) and (25) below and equation (28) satisfied by the 'inner solution' within a shock) depend only on the

presence of terms representing inertia, stresses transmitted between particles, gravity, and drag forces exerted between the fluid and the particle assembly, together with a comparison of the orders of magnitude of these terms. These results are best developed from the momentum balances, and we choose those postulated by Anderson & Jackson (1967), but we emphasize that our conclusions would not be changed significantly if these were replaced by other variants on these equations which have been suggested.

In terms of local mean variables, then, the one-dimensional momentum balance for the fluid is assumed to take the form

$$\rho_{\mathrm{f}}(1-\phi)\left[\frac{\partial u}{\partial t}+u\frac{\partial u}{\partial x}\right]=-(1-\phi)\frac{\partial p}{\partial x}-nf+(1-\phi)\rho_{\mathrm{f}}g. \tag{4}$$

The corresponding momentum equation for the solids is

$$\rho\phi\left[\frac{\partial v}{\partial t}+v\frac{\partial v}{\partial x}\right]=-\phi\frac{\partial p}{\partial x}+nf+\phi\rho g-\frac{\partial \sigma}{\partial x}, \tag{5}$$

with

$$nf=(1-\phi)\beta(\phi,|u-v|)(u-v)+\phi C(\phi)\rho_{\mathrm{f}}\frac{\mathrm{d}(u-v)}{\mathrm{d}t}. \tag{6}$$

Here u and v are the x-components of velocity for the suspending fluid and the particles, respectively; ρ and ρ_{f} are the densities of the solid and the fluid, respectively; p is the pressure for the fluid; σ is the stress transmitted by interactions between solid particles; and nf accounts for the fluid-particle interaction force arising from the relative motion. The first term in (6) represents a drag force exerted by the fluid on the particles and the second term a virtual mass force proportional to the mass of fluid displaced by a particle and the relative acceleration. Since the drag force must become proportional to $(u-v)$ at sufficiently low Reynolds number, the function β depends only on ϕ when $|u-v|$ is small; the virtual mass coefficient, C, whose value would be $\frac{1}{2}$ for an isolated spherical particle, is expected to depend on the volume fraction ϕ. There is no knowledge of the way in which the virtual mass coefficient varies with concentration, nor is there a unique form for the rate of change of the relative velocity. An acceptable definition of the relative acceleration is given by Murray (1965)

$$\frac{\mathrm{d}(u-v)}{\mathrm{d}t}=\left(\frac{\partial u}{\partial t}+u\frac{\partial u}{\partial x}\right)-\left(\frac{\partial v}{\partial t}+v\frac{\partial v}{\partial x}\right). \tag{7}$$

Any two independent linear combinations of (4) and (5) will serve equally well. In particular, we might take (4) together with an equation obtained by multiplying (4) by $\phi/(1-\phi)$ and subtracting from (5). Substituting from (6) and (7) then yields the following equation

$$\rho\phi\left[1+\frac{C(\phi)}{1-\phi}\frac{\rho_{\mathrm{f}}}{\rho}\right]\left[\frac{\partial v}{\partial t}+v\frac{\partial v}{\mathrm{d}x}\right]-\rho_{\mathrm{f}}\phi\left[1+\frac{C(\phi)}{1-\phi}\right]\left[\frac{\partial u}{\partial t}+u\frac{\partial u}{\partial x}\right]$$
$$=\beta(\phi)(u-v)+(\rho-\rho_{\mathrm{f}})g\phi-\frac{\partial \sigma}{\partial x}. \tag{8}$$

Then, with C set equal to zero, the first term on the left-hand side represents the rate of change of momentum of the solids, while the second describes the action on the particles of pressure gradients associated with fluid accelerations. The first term on

the right-hand side is the drag force due to relative motion of the fluid and the particles, the second is the difference between gravity and buoyancy forces, and the third represents the force due to a gradient in the stress σ transmitted directly between the particles. In uniform sedimentation only the first two terms on the right-hand side of (8) remain. Since the total flux must vanish, the fluid velocity u is related to v by

$$u = -\frac{\phi v}{1-\phi}. \tag{9}$$

and the drag coefficient $\beta(\phi)$ to the sedimentation velocity $U(\phi)$ by

$$\beta(\phi) = \frac{(\rho-\rho_f)\, g\phi(1-\phi)}{U(\phi)}. \tag{10}$$

This can be used to eliminate u and $\beta(\phi)$ from (8). Furthermore, assuming that the stress transmitted between particles depends only on ϕ, we can write $\sigma = \sigma(\phi)$, and hence

$$\frac{\partial \sigma}{\partial x} = \left(\frac{\mathrm{d}\sigma}{\mathrm{d}\phi}\right)\frac{\partial \phi}{\partial x}. \tag{11}$$

Equation (11) together with (8), (9), (10) and the continuity equation then constitute a theory of sedimentation in concentrated suspensions.

3. Conditions at a discontinuity

We now ask whether the above equations admit solutions in which the variables change very rapidly over an interval of x small with respect to the initial depth of the suspension. If so, these correspond to 'shocks' on the scale of the suspension as a whole, and the 'inner' solutions describe the structure of these shocks. These solutions then determine the nature of the jumps in the variables which may occur across the shock.

Before examining the inner solutions and their bearing on the existence of shocks it is valuable to re-write (8) in dimensionless terms. For this purpose, the natural lengthscale is L, the initial depth of the suspension, and the natural velocity scale is v_t, the terminal settling velocity of an isolated particle in an infinite body of fluid. Accordingly we define dimensionless variables as

$$x^* = \frac{x}{L}, \quad t^* = \frac{tv_t}{L}, \quad u^* = \frac{u}{v_t}, \quad v^* = \frac{v}{v_t}, \quad U^* = \frac{U(\phi)}{v_t},$$

so that (8) combined with (9) and (10) becomes

$$\frac{v_t^2}{gL}\left\{\left(1+\frac{C(\phi)}{1-\phi}\frac{\rho_f}{\rho}\right)\left(\frac{\partial v^*}{\partial t^*}+v^*\frac{\partial v^*}{\partial x^*}\right)-\frac{\rho_f}{\rho}\left(1+\frac{C(\phi)}{1-\phi}\right)\left(\frac{\partial u^*}{\partial t^*}+u^*\frac{\partial u^*}{\partial x^*}\right)\right\}$$
$$= \left(1-\frac{\rho_f}{\rho}\right)\left(1-\frac{v^*}{U^*(\phi)}\right)-\frac{1}{\phi}\frac{\mathrm{d}\sigma/\mathrm{d}\phi}{\rho g L}\frac{\partial \phi}{\partial x^*}. \tag{12}$$

This expression contains two dimensionless parameters, $\rho_f/\rho, v_t^2/gL$, and two dimensionless functions of ϕ, $(\mathrm{d}\sigma/\mathrm{d}\phi)/\rho gL$ and $C(\phi)$. The first parameter is simply the density ratio, while the second represents the ratio of a lengthscale v_t^2/g, associated with the inertial terms, to the geometric lengthscale L. The first function represents the ratio of a lengthscale $(\mathrm{d}\sigma/\mathrm{d}\phi)/\rho g$, associated with stresses transmitted between the particles, to the geometric lengthscale L.

The possibility of a shock, that is, an $O(1)$ change in ϕ over a distance very small compared with L, exists only if v_t^2/gL and $(\mathrm{d}\sigma/\mathrm{d}\phi)/\rho gL$, are small compared with unity. Then the structure of the shock can be obtained from pseudo-steady solutions of (12) and the associated continuity equation for the particles, in the rest frame of the shock. This will provide 'inner solutions', valid in the limit as the shock thickness shrinks to zero, which must match 'outer solutions' in adjacent regions where the concentration varies relatively smoothly (Rhee *et al.* 1986; Davis & Russel 1988). This matching process should determine criteria for the existence of shocks. The most obvious inner regions, between the clear fluid and the settling region or the settling zone and the sediment, appear on the scale of the suspension as jumps in concentration at the surface of the settling region, or at the surface of the rising sediment. But shock-like behaviour may also be possible within the settling zone depending on the curvature of the flux curve $\phi U(\phi)$ and the initial condition.

Outside shock layers we assume that stress gradients and inertial terms are small enough to be negligible; then (12) simply balances drag forces and the buoyant weight, and the particles descend with the sedimentation velocity $U(\phi)$. Thus, outer solutions satisfy the Kynch equation (2).

3.1. *Shocks within the suspension region*

Let us consider the possibility of a shock separating two regions of slowly varying ϕ, namely ϕ_1 above and ϕ_2 below, with corresponding dimensionless sedimentation velocities $U_1 = U^*(\phi_1)$ and $U_2 = U^*(\phi_2)$, respectively. (From now on, the asterisks will be omitted for simplicity and all variables will be assumed to be dimensionless.) Viewing this shock from a frame of reference which moves with it, with a dimensionless velocity V (positive upward), we then can apply the pseudo-steady state hypothesis. In the frame of the shock, the dimensionless continuity condition for the particles reduces to

$$\phi(v+V) = \phi_1(U_1+V) = \phi_2(U_2+V), \tag{13}$$

and for the liquid to

$$(1-\phi)(u+V) = (1-\phi_1)(u_1+V) = (1-\phi_2)(u_2+V), \tag{14}$$

where u and v are velocities relative to the rest frame and ϕ is the volume fraction of the solid, at any point within the shock layer. Similarly, (12) becomes

$$\frac{v_t^2}{gL}\left\{\left(1+\frac{C(\phi)}{1-\phi}\frac{\rho_f}{\rho}\right)(v+V)\frac{\partial v}{\partial x}-\frac{\rho_f}{\rho}\left(1+\frac{C(\phi)}{1-\phi}\right)(u+V)\frac{\partial u}{\partial x}\right\} = \left(1-\frac{\rho_f}{\rho}\right)\left(1-\frac{v}{U(\phi)}\right)-\frac{1}{\rho gL}\frac{1}{\phi}\left(\frac{\mathrm{d}\sigma}{\mathrm{d}\phi}\right)\frac{\partial\phi}{\partial x}. \tag{15}$$

Combining (13) and (14) yields

$$v = \frac{(\phi_2-\phi)\phi_1 U_1+(\phi-\phi_1)\phi_2 U_2}{\phi(\phi_2-\phi_1)}, \tag{16}$$

$$V = \frac{\phi_1 v_1-\phi_2 v_2}{\phi_2-\phi_1}, \tag{17}$$

$$v+V = \frac{\phi_1\phi_2(U_1-U_2)}{\phi(\phi_2-\phi_1)}, \tag{18}$$

$$u+V = \frac{(1-\phi_1)\phi_2 U_2-(1-\phi_2)\phi_1 U_1}{(1-\phi)(\phi_1-\phi_2)}, \tag{19}$$

which imply that

$$\frac{\partial v}{\partial x} = -\frac{v+V}{\phi}\frac{\partial \phi}{\partial x}, \tag{20}$$

$$\frac{\partial u}{\partial x} = \frac{u+V}{(1-\phi)}\frac{\partial \phi}{\partial x}. \tag{21}$$

Then (15), (16), (20) and (21) combine to give a single equation which determines the variation in particle concentration within the shock

$$\left[\frac{1}{\rho g L}\frac{\mathrm{d}\sigma}{\mathrm{d}\phi} - \frac{v_t^2}{gL}h(\phi)\right]\frac{\partial \phi}{\partial x} = \left(1-\frac{\rho_f}{\rho}\right)\left[\frac{(\phi_2-\phi_1)\phi U - (\phi_2-\phi)\phi_1 U_1 - (\phi-\phi_1)\phi_2 U_2}{(\phi_2-\phi_1)U}\right], \tag{22}$$

where

$$h(\phi) = \left(1+\frac{C(\phi)}{1-\phi}\frac{\rho_f}{\rho}\right)(v+V)^2 + \frac{\rho_f}{\rho}\frac{\phi}{1-\phi}\left(1+\frac{C(\phi)}{1-\phi}\right)(u+V)^2, \tag{23}$$

representing the contribution of the inertial effects, is always positive.

The right-hand side of (22) is a product of factors whose magnitudes are of order unity. Thus the length of the interval of x, over which a significant change in ϕ occurs, is proportional to the factor in brackets on the left-hand side. If the magnitude of this is $\ll 1$, then ϕ may change significantly over a distance which is very small compared with the total depth of the suspension. Then recognizable shocks may occur with a 'thickness' which depends on the parameters $(\mathrm{d}\sigma/\mathrm{d}\phi)/\rho g$ and v_t^2/g. If

$$\frac{v_t^2}{gL} \ll \frac{\mathrm{d}\sigma/\mathrm{d}\phi}{\rho g L} \ll 1, \tag{24}$$

a shock may exist with thickness of the order of $(\mathrm{d}\sigma/\mathrm{d}\phi)/\rho g$ determined by the stress gradient terms alone (since $h(\phi)$ is of order unity), while inertial effects are negligible, even within the shock. On the other hand, if

$$\frac{\mathrm{d}\sigma/\mathrm{d}\phi}{\rho g L} \ll \frac{v_t^2}{gL} \ll 1, \tag{25}$$

a shock again may exist, but now its thickness is of the order of v_t^2/g determined by inertial effects, while interparticle forces may be neglected, even within the shock. If either of the parameters is not $\ll 1$, then recognizable shocks cannot occur.

These observations alone resolve the difficulties associated with inertia raised by Dixon (1977). While it is true, as Dixon points out, that inertial terms can never be neglected in an ideal shock where conditions change discontinuously across a geometric surface, real shocks have a finite, though small, thickness. When the inequalities (24) are satisfied (as for sedimentation of small particles) the thickness of the shock is determined by interparticle forces, and terms associated with acceleration over this lengthscale are negligible in comparison. In principle the opposite situation, characterized by the inequalities (25), can also arise, but with such large inertial effects it is doubtful that the system can be described adequately by the present model, which assigns a unique particle velocity to each position.

The variation of ϕ within the shock layer can, in principle, be found by integrating (22). However the information needed to interpolate between two outer solutions can be obtained without doing this explicitly, simply by examining the geometry of the sedimentation curve. The values of ϕ outside the shock, and adjacent to it, correspond to two points on the sedimentation curve; for example, points 1 and 2,

or points 3 and 4 on figure 1. From (17) the velocity of a shock separating these two conditions, supposing that one may exist, equals minus the slope of the chord joining the points. For points 1 and 2, as drawn, the chord lies entirely below the sedimentation curve, while for points 3 and 4 it lies entirely above.

Now, for any value of ϕ along the chord, the bracketed quantity on the right-hand side of (22) represents the vertical distance between the chord and the sedimentation curve, counted positive if the chord lies below the curve. Thus, in the common situation corresponding to inequalities (24), equation (22) shows that $\mathrm{d}\phi/\mathrm{d}x$ will be positive when the chord lies below the sedimentation curve and negative when it lies above. This is indicated by the arrows drawn on the chords in figure 1. When the chord lies below the curve, it follows that ϕ increases on moving down through the shock, and we have a compression shock. Conversely, when the chord lies above the curve, we have a rarefaction shock. If the chord intersects the curve at some intermediate point, a shock between conditions represented by the end points is not possible, since any interval of ϕ containing the intermediate intersection point is seen from (22) to correspond to an unbounded interval of x. These conditions are consistent with those of Lax (1973) and the interparticle stress provides a physical basis for the selection of shocks. The same geometric interpretation can also be applied to shocks which occur at the surface of the rising sediment.

3.2. *The surface of the rising sediment*

Kynch's theory accounts for neither inertial effects nor stress gradients, leading to discontinuities at the surface of the rising sediment. We now examine the case where inertial forces can be neglected as in (24). Under these circumstances, let us look at a layer near the surface of the rising sediment, within which $\phi = \phi_{\mathrm{m}}$. We consider the case in which this layer is thin, so that it can be regarded as a shock and the pseudo-steady state approximation can be invoked. Then (15) reduces to

$$\frac{\mathrm{d}\sigma}{\mathrm{d}\phi}\frac{\partial\phi}{\partial x} = (\rho-\rho_{\mathrm{f}})\,gL\phi\left[1-\frac{v}{U}\right]. \tag{26}$$

Viewed from the frame of reference of the sediment surface rising with speed $(\mathrm{d}L/\mathrm{d}t)$, the condition of continuity of flux at the surface is

$$\phi_{\mathrm{m}}\frac{\mathrm{d}L}{\mathrm{d}t} = \phi\left[v+\frac{\mathrm{d}L}{\mathrm{d}t}\right]. \tag{27}$$

Eliminating v between (26) and (27) leads to a differential equation

$$\frac{\partial\phi}{\partial x} = \left[\phi U-(\phi_{\mathrm{m}}-\phi)\frac{\mathrm{d}L}{\mathrm{d}t}\right]\frac{(\rho-\rho_{\mathrm{f}})\,gL}{U}\frac{\partial\phi}{\partial\sigma}, \tag{28}$$

whose solution must be matched to the outer solutions corresponding to the descending suspension and the rising sediment.

Since ϕ is larger for the rising sediment than for the suspension, matching is possible only if $\mathrm{d}\phi/\mathrm{d}x \geqslant 0$ throughout the inner solution, which in turn requires that

$$\phi U-(\phi_{\mathrm{m}}-\phi)\frac{\mathrm{d}L}{\mathrm{d}t} \geqslant 0, \tag{29}$$

for all values of ϕ between ϕ_{m} and that corresponding to the descending suspension. This situation is represented in figure 1, where ϕ_{α} corresponds to the suspension.

From (27), $\mathrm{d}L/\mathrm{d}t$ is the slope of the chord joining the point (α), representing the suspension, to the point ($\phi_\mathrm{m}, 0$), representing the sediment. Furthermore

$$\phi U - (\phi_\mathrm{m} - \phi)\,(\mathrm{d}L/\mathrm{d}t)$$

is just the vertical separation between this chord and the sedimentation curve, counted positive when the chord lies below the curve, so the above condition for matching requires that this chord lies below the sedimentation curve over its whole length.

Now consider a line through ($\phi_\mathrm{m}, 0$) which is tangent to the sedimentation curve at point (b) and intersects it at a second point (a). For suspensions with volume fractions of solid between zero and ϕ_a (e.g. ϕ_α), or between ϕ_b and ϕ_m (e.g. ϕ_β), the above condition is satisfied by the chord joining the point representing the suspension to ($\phi_\mathrm{m}, 0$), so these suspensions can deposit directly on the rising sediment surface. For suspension volume fractions in the interval $[\phi_a, \phi_b]$, however, the chord joining the point representing the suspension to ($\phi_\mathrm{m}, 0$) does not lie entirely below the sediment curve, and matching is not possible. Direct deposition of suspensions of this class on the sediment surface is, therefore, impossible.

The problem now reduces to finding an outer solution satisfying the Kynch equation (2), which is consistent with the initial state of the suspension and yields values of ϕ at the surface of the sediment which lie in the intervals $[0, \phi_a]$ or $[\phi_b, \phi_\mathrm{m}]$. When the forces associated with the interparticle stress dominate, as in (24), it is possible to resolve all ambiguities in constructing solutions of the Kynch type for the settling region, and match them to solutions for the sediment, using only intermediate shocks satisfying the above conditions in addition to the shock at the sediment surface.

4. Complete solution for sedimentation of an initially uniform suspension

Having explored the variety of possible shocks and identified the physical characteristics of particles and suspending fluid for which inertial effects can be neglected, we can construct the complete solution of the sedimentation problem for an initially uniform suspension of any volume fraction ϕ_0, together with appropriate combinations of Kynch theory and shock conditions. The different cases, which are all identified in the existing literature (Rhee *et al.* 1986), appear for a typical flux curve which presents one point of inflexion (i), at $\phi = \phi_i$, and where the points (a) and (b) are the same as in figure 1.

(a) $0 < \phi_0 < \phi_a$. A direct jump is possible at the sediment surface from the value ϕ_0 to the value ϕ_m, so only one stage of settling occurs. The rate of fall of the descending suspension is constant and equal to $U(\phi_0)$. This situation is shown in figure 1 where the initial condition is represented by the point (α).

(b) $\phi_b < \phi_0 < \phi_\mathrm{m}$. Once again, no intermediate shock is necessary and direct deposition on the rising sediment is possible. This initial condition is represented by the point (β) in figure 1.

(c) $\phi_i < \phi_0 < \phi_b$. Direct contact between the suspension at the initial concentration and the sediment surface is not possible, nor can any acceptable shock propagate to regions which can contact the rising sediment. Therefore we must construct a solution in which ϕ changes continuously from ϕ_0 to ϕ_b, through a fan of characteristics from the origin. At point (b), the characteristics are parallel to the

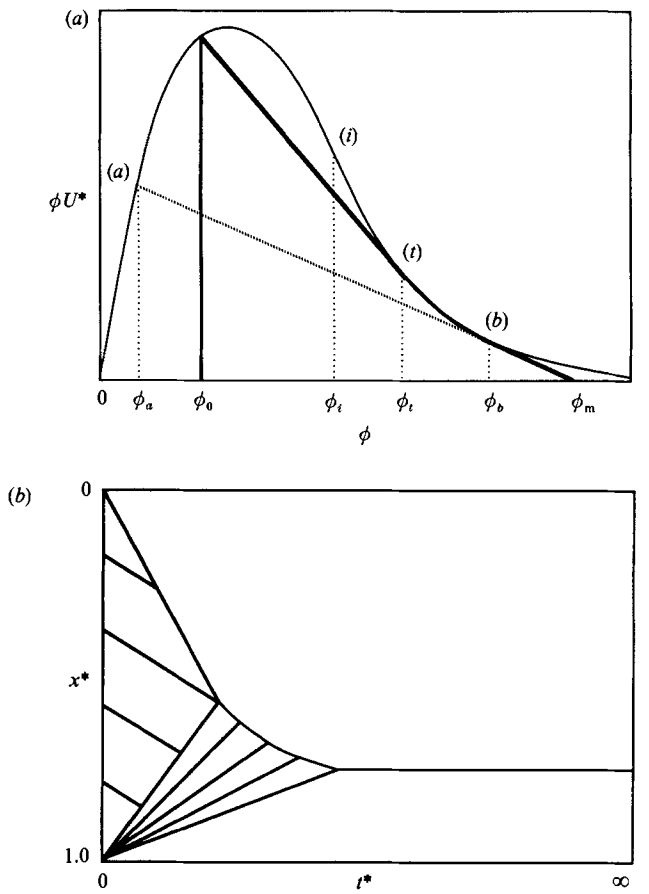

FIGURE 2. (*a*) Schematic of sedimentation with $\phi_a < \phi_0 < \phi_i$, showing the associated discontinuities. (*b*) Contours of constant density for $\phi_a < \phi_0 < \phi_i$.

surface of the rising sediment and (*b*) is acceptable as a point representing material in contact with the sediment surface. The fan cannot extend to $\phi_b < \phi < \phi_m$ since then the line representing the sediment surface is steeper than the characteristics. For this type of situation, the descent of the top of the suspension slows down before all particles have joined the sediment. This is referred to as a falling rate period.

(*d*) $\phi_a < \phi_0 < \phi_i$. Once again, direct contact with the sediment surface is not possible nor can a compression shock be constructed leading to a condition such that $\phi_b < \phi < \phi_m$, from which the jump to the sediment can be made. However, we can construct a compression shock to a point such that $\phi_i < \phi < \phi_b$ and then complete the solution as in (*c*). In order to have the flux balanced, this shock must be incident tangentially on the sedimentation curve at a point (*t*) between ϕ_i and ϕ_b, as shown in figure 2. If ϕ_0 represents the initial value with a compression shock from ϕ_0 to ϕ_t, then a fan of characteristics determines ϕ in the interval $[\phi_t, \phi_b]$ while at ϕ_b the material can contact the rising sediment surface (figure 2). Once again there is a falling rate period. This case corresponds to what Been & Sills (1981) have observed and called a transition zone between dispersion and sediment.

5. The numerical scheme

When inequalities (24) or (25) are not satisfied there are no recognizable shocks, and the above method of solving the sedimentation problem fails. However, direct numerical solution of the equations of motion is still available, and we shall use it to illustrate the nature of the solution in general, and show the convergence to the above results for appropriate parameter values. In particular, we shall assume that $v_t^2/gL \ll (\mathrm{d}\sigma/\mathrm{d}\phi)/\rho gL$, but not that $(\mathrm{d}\sigma/\mathrm{d}\phi)/\rho gL \ll 1$. Then the dimensionless momentum equation (12) reduces to

$$v = U(\phi)\left[1 - \frac{\mathrm{d}\sigma/\mathrm{d}\phi}{(\rho-\rho_f)gL\phi}\frac{\partial\phi}{\partial x}\right], \tag{30}$$

while the dimensionless continuity equation becomes

$$\frac{\partial\phi}{\partial t} + \frac{\partial}{\partial x}\left[U(\phi)\left(\phi - \frac{\mathrm{d}\sigma/\mathrm{d}\phi}{(\rho-\rho_f)gL}\frac{\partial\phi}{\partial x}\right)\right] = 0. \tag{31}$$

Together with the no-flux conditions at the top and bottom of the sedimentation column, these constitute a complete description of the process. Numerical solution of the problem makes no *a priori* distinction between clear liquid, suspension and sediment, and the interfaces between these regions, though no longer sharp, should appear in the solutions as recognizable features of the concentration profile throughout the column. Then, by repeating the computations for successively decreasing values of $(\mathrm{d}\sigma/\mathrm{d}\phi)/\rho gL$, it should be possible to see convergence towards the different types of solution shown in figure 2. Thus, the computations will serve the dual purpose of confirming the validity of the reasoning leading to the solutions of figure 2, and showing how the actual situation deviates from these ideal solutions as the magnitude of interparticle forces increases.

To proceed further requires specific forms for the functions $U(\phi)$ and $\sigma(\phi)$. The next section discusses appropriate forms for hard spheres, to exemplify stable dispersions, and for flocculated networks.

6. Constitutive relations

Hard spheres provide a useful and realizable model for stable colloidal dispersions for which simple, but robust constitutive relations for U and σ can be constructed from information in the literature. For example, Batchelor (1972) derived the dilute limit for the sedimentation velocity as

$$U(\phi) = 1 - 6.55\phi + O(\phi^2) \tag{32}$$

for low-Reynolds-number motion. Experimental results at higher concentrations reported by Buscall *et al.* (1982) for aqueous polystyrene latices at 10^{-3} M NaCl and deKruif, Jansen & Vrij (1987) for silica spheres in cyclohexane roughly follow the empirical equation

$$U(\phi) = (1-\phi)^p, \tag{33}$$

with $5.8 \leqslant p \leqslant 6.6$. Hence we describe the sedimentation velocity of hard spheres at finite volume fractions through (33) with $p = 6.55$ to conform with both the dilute limit and values measured for $\phi \geqslant 0.4$.

For stable dispersions of small particles the transmitted stress $\sigma(\phi)$ is equivalent

to the osmotic pressure Π. The origin of this relationship can be illustrated by considering a dispersion with a monotonically varying volume fraction, e.g. decreasing upward. In the absence of an external field, such a spatially varying concentration represents a non-equilibrium state. Consequently, both particles and fluid molecules experience forces, proportional to the gradients in their respective chemical potentials (Batchelor 1976). But the osmotic pressure of a solute, or a colloidal particle, is directly proportional to the chemical potential of the solvent. Hence the thermodynamic force, or equivalently the stress, can be written for spheres of radius a as

$$\begin{aligned}\sigma(\phi) &= \Pi \\ &= \frac{3kT}{4\pi a^3}\phi Z(\phi),\end{aligned} \tag{34}$$

with $Z(\phi)$ known as the compressibility factor and kT the thermal energy. In the dilute limit $Z(\phi) = 1+4\phi+O(\phi^2)$ for hard spheres. Near random close packing molecular dynamics simulations indicate that $Z(\phi)$ diverges as

$$Z(\phi) = \frac{1.85}{\phi_m - \phi}, \tag{35}$$

with $\phi_m = 0.64$ (Woodcock 1981). Equation (35) suffices for the semi-quantitative purposes of this work.

For flocculated suspensions, the physical situation is more complex. In very dilute systems flocculation increases the sedimentation rate since finite flocs behave as larger, discrete sedimenting units. At higher concentrations of interest here, however, interactions produce a gelation phenomenon in which individual flocs join together into a volume-filling network (Michaels & Bolger 1962). Thus the hydrodynamic problem involves flow through a network of spherical particles as described by Brinkman (1947). His model of the porous medium as a single sphere embedded in an effective medium determined the permeability as

$$k = \frac{2a^2}{9\phi}\frac{(2-3\phi)^2}{3\phi+4+3(8\phi-3\phi^2)^{\frac{1}{2}}}. \tag{36}$$

With this the argument following (8) establishes

$$U(\phi) = \frac{9\phi}{2a^2}k. \tag{37}$$

The artificial zero at $\phi = \frac{2}{3}$ lies above random close packing and is not significant.

The stress σ within a flocculated network cannot exceed the compressive yield stress. Otherwise the network collapses to a higher volume fraction capable of bearing the load. Though no theory exists, the empirical expression

$$\sigma(\phi) = \frac{\sigma_0\phi^n}{\phi_m - \phi}, \tag{38}$$

with $2 \leqslant n \leqslant 5$, $\phi_m = 0.64$ and $\sigma_0 =$ constant mimics the experimental data available for the compressive yield stress of several flocculated dispersions (Buscall & White 1987). This pseudo-static form for σ implies that the rate of consolidation is limited by the resistance to moving fluid through the network and not by the resistance to moving particles relative to each other.

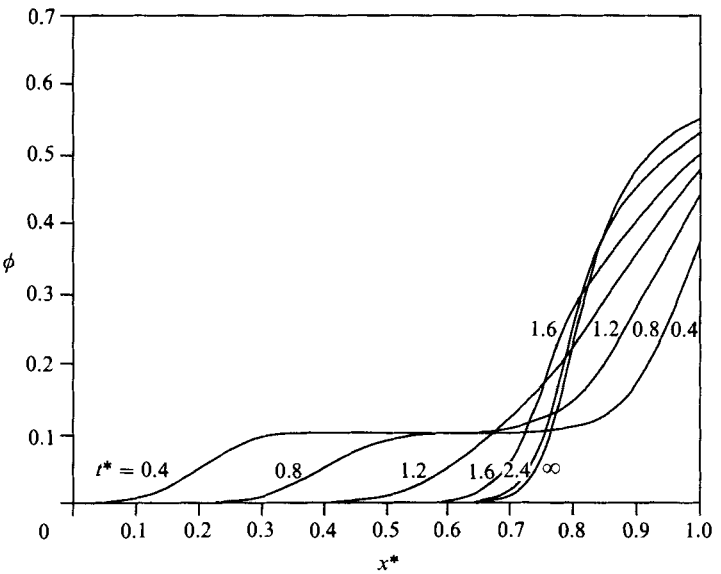

FIGURE 3. Concentration profiles at various times for $\phi_0 = 0.1$ and $Pe = 85$ for stable suspension.

7. Numerical results

For the numerical treatment, standard techniques for the solution of partial differential equations may be used, and an implicit method was chosen for stability reasons. The integration itself is done with GEARB, developed by Hindmarsh (1975), in double precision. This package is especially suited to stiff problems. We used, for the solution of this initial-value problem, the classical three-point second-order finite difference approximations, a relative error of 10^{-5} and a spatial step size of 5×10^{-5}. GEARB adjusts the temporal step size to achieve this specific error.

7.1. *The hard sphere model*

The equation that governs the sedimentation behaviour is found by combining (31), (33), (34) and (35), so for $0 \leqslant x \leqslant 1$

$$\frac{\partial \phi}{\partial t} + \frac{\partial}{\partial x}\left[(1-\phi)^{6.55}\left(\phi - \frac{1}{Pe}\frac{1.85\phi_m}{(\phi_m-\phi)^2}\frac{\partial \phi}{\partial x}\right)\right] = 0 \tag{39}$$

must be satisfied.

The boundary conditions for a closed container are no flux at both the top and the bottom, i.e.

$$\frac{\partial \phi}{\partial x} = \frac{Pe\phi(\phi_m-\phi)^2}{1.85\phi_m} \quad \text{at } x = 0, 1, \tag{40}$$

where

$$Pe = \tfrac{4}{3}\pi a^3 \frac{(\rho-\rho_f)gL}{kT} \tag{41}$$

is the ratio of gravitational potential to the magnitude of the osmotic pressure. It is therefore large when transmitted stresses are small, and vice versa.

The initial condition is chosen such that $\phi_a < \phi_0 < \phi_i$, which corresponds to the

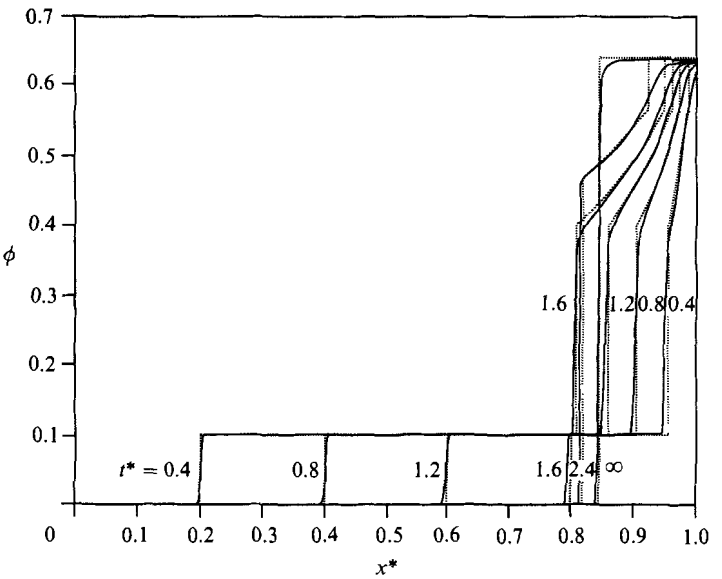

FIGURE 4. Concentration profiles at various times for $\phi_0 = 0.1$ and $Pe = 8500$ for stable suspension. The dotted lines correspond to $Pe \to \infty$ (Kynch case).

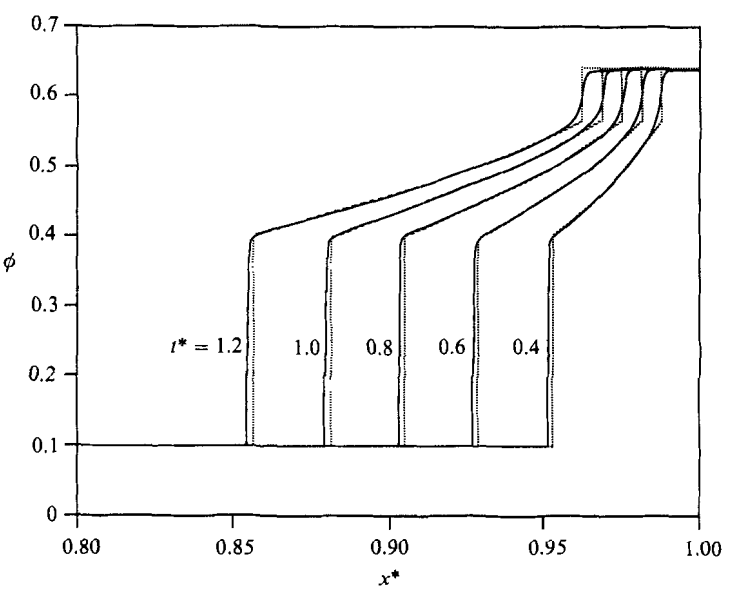

FIGURE 5. Concentration profiles at various times for $\phi_0 = 0.1$ and $Pe = 1.7 \times 10^5$ for stable suspension, with $Pe \to \infty$ (Kynch case) represented by the dotted lines.

most complex case at $Pe = \infty$, where an intermediate shock develops, separated by a region of continuously varying volume fraction from a second shock at the surface of the sediment. For the flux curve described previously, an appropriate initial value is $\phi_0 = 0.1$. In order to study the influence of the interparticle forces and show that these are responsible for the mechanics of settling in the transition zones, we vary the Péclet number from 85 to 1.7×10^5. Larger values require a very long integration time.

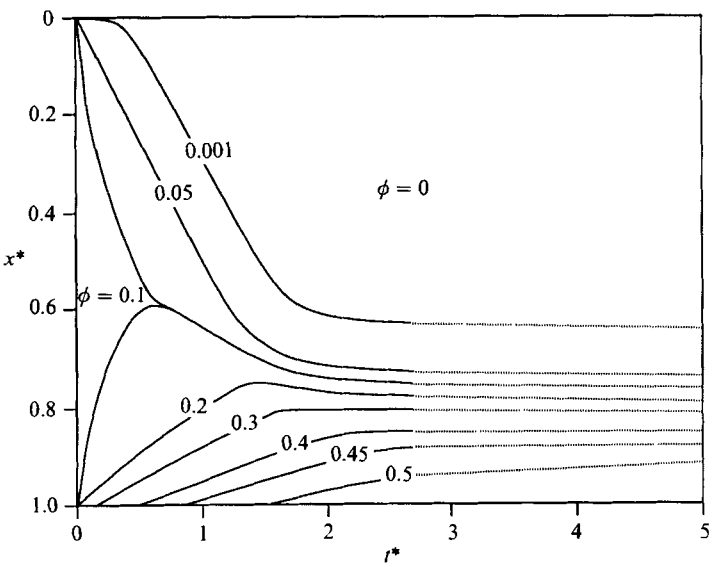

FIGURE 6. Settling behaviour showing lines of constant density for $Pe = 85$ for stable suspension.

Figures 3 and 4 demonstrate the smooth variation in volume fraction for various times. At $Pe = 85$ (figure 3), ϕ varies smoothly from top to bottom and remains rather smaller at the bottom than ϕ_m, indicating the influence of significant interparticle forces throughout the column. As Pe increases to 8500 (figure 4) the interface in contact with the supernatant fluid becomes sharper, and a uniform zone of constant ϕ now clearly appears. The bottom sediment builds up with a much sharper surface, but does not yet reach maximum packing and a large concentration gradient separating the falling rate period from the uniform suspension appears. Also, the top of the suspension and the intermediate jump separating the uniform suspension from the falling rate period closely resemble those predicted by the Kynch solution (dotted curves on figure 4). The final case treated, $Pe = 1.7 \times 10^5$ (figure 5) corresponds well to $Pe = \infty$ (Kynch case) shown by the dotted lines. The transition from the uniform suspension at $\phi = 0.1$ to the falling rate region with $\phi = 0.4$ now resembles a shock, and the steep parts of the curves leading to $\phi = 0.64$ approximate the jump at the sediment surface in the Kynch solution. The fact that this last is not a discontinuity comes from the form of $\sigma(\phi)$. If we had chosen a function which remained zero near $\phi = \phi_m$, then increased rapidly toward ∞ at ϕ_m, the Kynch solution would be simulated very accurately. Nonetheless, these results clearly verify the validity of the Kynch solution as a limiting case for $Pe \to \infty$, and show how this limit is approached.

Figures 6 and 7 represent curves of constant ϕ in the (x,t)-plane for the Péclet numbers studied previously. We note that the line of constant density $\phi = 0.05$ at the upper surface always follows the Kynch case represented by the characteristic of slope $-U(\phi_0)$. But the time for equilibrium to be reached is much greater than predicted by Kynch, even at very large Péclet. The evolution of the lines of constant density of the rising sediment indicates, at low Péclet number, quite a different behaviour. We see that the zone of constant concentration remains only for a short time. As $Pe \to \infty$ the thickness of the intermediate region decreases to approach a

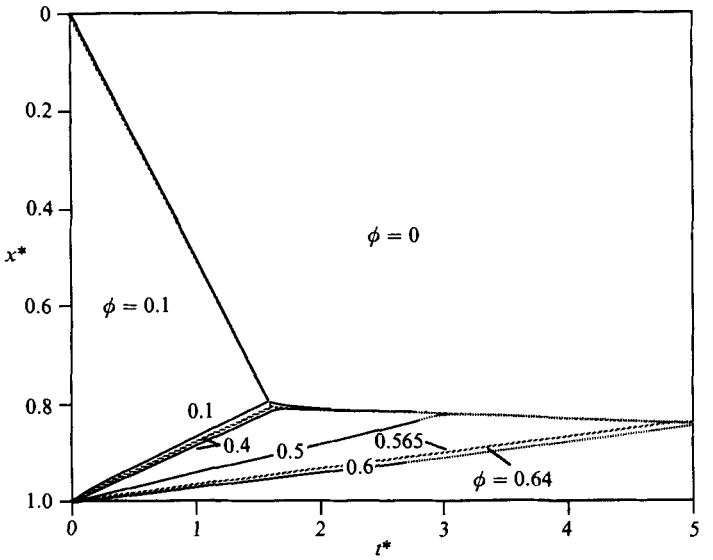

FIGURE 7. Settling behaviour showing lines of constant density for $Pe = 8500$ for stable suspension. $Pe \to \infty$ (Kynch case) in dashed lines.

true discontinuity and the concentration of the sediment approaches close packing, as the solutions collapse to the Kynch case represented by the dashed lines in figure 7. For flocculated suspensions, the physical situation is more complex.

7.2. *The flocculated model*

In this case three regions can be distinguished within the sedimenting dispersion. As with stable dispersions a clear fluid layer forms above a uniform dispersion at the initial volume fraction. At the interface $x = x_1(t)$ the stress within the dispersion is zero but below that it increases linearly with depth. The point $x = x_2(t)$ at which the stress reaches the compressive yield value marks the top of the sediment. From there to the bottom the stress retains the local yield value while the volume fraction increases monotonically with depth. Thus the problem is to calculate the positions of the boundaries $x_1(t)$ and $x_2(t)$ and $\phi(x,t)$ for $x_2(t) \leqslant x \leqslant 1$. In the uniform region, $\phi = \phi_0$ and the stress varies as

$$\sigma(x) = \frac{x(t)-x_1(t)}{x_2(t)-x_1(t)}\sigma(\phi_0). \tag{42}$$

Then

$$\frac{\mathrm{d}\sigma}{\mathrm{d}x} = \frac{\sigma(\phi_0)}{x_2(t)-x_1(t)}, \tag{43}$$

and all particles within $x_1(t) < x < x_2(t)$ fall with the same velocity,

$$\frac{\mathrm{d}x_1}{\mathrm{d}t} = U(\phi_0)\left[1-\frac{1}{(\rho-\rho_\mathrm{f})gL\phi_0}\frac{\sigma(\phi_0)}{x_2(t)-x_1(t)}\right]. \tag{44}$$

In the region $x_2(t) < x < 1$, the governing equation for the consolidating sediment is

$$\frac{\partial\phi}{\partial t}+\frac{\partial}{\partial x}\left[\frac{(2-3\phi)^2}{3\phi+4+3(8\phi-3\phi^2)^{\frac{1}{2}}}\left(\phi-\frac{\mathrm{d}\sigma/\mathrm{d}\phi}{(\rho-\rho_\mathrm{f})gL}\frac{\partial\phi}{\partial x}\right)\right] = 0, \tag{45}$$

subject to the zero flux condition at the bottom, $x = 1$. Continuity of the volume fraction and flux across $x = x_2(t)$ requires $\phi(x_2) = \phi_0$ and

$$\frac{\partial \phi}{\partial x}(x_2) = \frac{1}{x_2(t) - x_1(t)} \frac{\sigma(\phi_0)}{\mathrm{d}\sigma/\mathrm{d}\phi_{|\phi=\phi_0}}. \tag{46}$$

Since ϕ is a function of x and t but constant at $x = x_2(t)$, $x_2(t)$ can be obtained upon integration of

$$\frac{\mathrm{d}x_2}{\mathrm{d}t} = -\frac{\partial \phi/\partial t_{|x=x_2}}{\partial \phi/\partial x_{|x=x_2}}. \tag{47}$$

Thus the coupled equations (44)–(47) determine $x_1(t), x_2(t)$ and $\phi(x, t)$ for $0 < x < 1$.

This moving-boundary problem is most conveniently solved by transforming the variable integration domain $x_2(t) < x < 1$ into the fixed one $0 < \xi < 1$ with

$$\xi(t) = \frac{x(t) - x_2(t)}{1 - x_2(t)}. \tag{48}$$

Transformation of (44), (45) and (47) produces a system of three equations,

$$\frac{\partial \phi}{\partial t} + \frac{\xi - 1}{1 - x_2} \frac{\mathrm{d}x_2}{\mathrm{d}t} \frac{\partial \phi}{\partial \xi} + \frac{1}{1 - x_2} \frac{\partial}{\partial \xi} \left[U(\phi) \left(\phi - \frac{1}{1 - x_2} \frac{\mathrm{d}\sigma/\mathrm{d}\phi}{(\rho - \rho_f) g L} \frac{\partial \phi}{\partial \xi} \right) \right] = 0, \tag{49}$$

$$\frac{\mathrm{d}x_1}{\mathrm{d}t} = U(\phi_0) \left[1 - \frac{1}{x_2 - x_1} \frac{\sigma(\phi_0)}{(\rho - \rho_f) g L \phi_0} \right], \tag{50}$$

$$\frac{\mathrm{d}x_2}{\mathrm{d}t} = \frac{\dfrac{\partial}{\partial \xi} \left[U(\phi) \left(\phi - \dfrac{1}{1 - x_2} \dfrac{\mathrm{d}\sigma/\mathrm{d}\phi}{(\rho - \rho_f) g L} \dfrac{\partial \phi}{\partial \xi} \right) \right]_{|\xi=0}}{\left(\dfrac{\partial \phi}{\partial \xi} \right)_{|\xi=0}}, \tag{51}$$

which must be solved simultaneously with the initial conditions $x_1 = 0$, $x_2 = 1$, $\phi = \phi_0$ at $t = 0$ and the associated boundary conditions

$$\frac{\partial \phi}{\partial \xi} = \frac{1 - x_2}{x_2 - x_1} \frac{\sigma(\phi_0)}{\mathrm{d}\sigma/\mathrm{d}\phi_{|\phi=\phi_0}} \quad \text{at } \xi = 0, \tag{52}$$

from (46) and the analogue of (40), namely

$$\frac{\partial \phi}{\partial \xi} = \frac{(1 - x_2)(\rho - \rho_f) g L \phi}{\mathrm{d}\sigma/\mathrm{d}\phi} \quad \text{at } \xi = 1. \tag{53}$$

The nonlinearity of the system of equations makes a general solution extremely difficult if not impossible to obtain. Furthermore the initial conditions present a singularity at $t = 0$. To overcome this problem and start the numerical calculation, we derive a short time solution of the form

$$\phi(\xi, t) = \phi_0 + \phi_1(\xi, t), \tag{54}$$

with $\phi_1 \ll \phi_0$. Taylor series expansions of $U(\phi)$ and $\sigma(\phi)$ about $\phi = \phi_0$

$$U(\phi) = U_0 + \phi_1 U_0' + \ldots, \tag{55}$$

$$\frac{\mathrm{d}\sigma}{\mathrm{d}\phi} = \sigma_0' + \phi_1 \sigma_0'' + \ldots, \tag{56}$$

where the primes and double primes indicate the first and second derivatives with respect to ϕ_0 and the suffix 0 denotes the value of the associated functions at $\phi = \phi_0$, lead to the linearized forms of (49) and (51),

$$\frac{\partial \phi_1}{\partial t} + \frac{\xi - 1}{1 - x_2}\frac{\mathrm{d}x_2}{\mathrm{d}t}\frac{\partial \phi_1}{\partial \xi} + \frac{1}{1-x_2}\frac{\partial}{\partial \xi}\left[\left(\frac{\partial \phi U}{\partial \phi}\right)_{|0}\phi_1 - \frac{1}{1-x_2}\frac{U_0\sigma_0'}{(\rho-\rho_\mathrm{f})gL}\frac{\partial \phi_1}{\partial \xi}\right] = 0, \tag{57}$$

and

$$\frac{\mathrm{d}x_2}{\mathrm{d}t} = \left(\frac{\partial \phi U}{\partial \phi}\right)_{|0} - \frac{1}{1-x_2}\frac{U_0\sigma_0'(\partial^2\phi_1/\partial\xi^2)_{|\xi=0}}{(\rho-\rho_\mathrm{f})gL(\partial\phi_1/\partial\xi)_{|\xi=0}}. \tag{58}$$

Similar linearization of the boundary conditions, equations (52) and (53), gives

$$\frac{\partial \phi_1}{\partial \xi} = \frac{1-x_2}{x_2-x_1}\frac{\sigma(\phi_0)}{\sigma_0'} \quad \text{at } \xi = 0, \tag{59}$$

and

$$\frac{\partial \phi_1}{\partial \xi} + (1-x_2)\frac{(\rho-\rho_\mathrm{f})gL}{U_0\sigma_0'}\left[U_0\phi_0 + \left(\frac{\partial \phi U}{\partial \phi}\right)_{|0}\phi_1\right] \quad \text{at } \xi = 1. \tag{60}$$

For very short times, $x_2 - x_1 \sim 1$, permitting integration of (50) to give (Buscall & White 1987)

$$x_1(t) = U_0\left[1 - \frac{\sigma(\phi_0)}{(\rho-\rho_\mathrm{f})gL\phi_0}\right]t. \tag{61}$$

To integrate (58), we evaluate $\partial^2\phi_1/\partial\xi^2$ by noting that

$$\left(\frac{\partial^2\phi_1}{\partial x^2}\right)_{|x=1} = \lim_{x_2 \to 1}\frac{\left(\dfrac{\partial \phi_1}{\partial x}\right)_{|x=1} - \left(\dfrac{\partial \phi_1}{\partial x}\right)_{|x=x_2}}{1-x_2}, \tag{62}$$

which can be rewritten in terms of ξ as

$$\left(\frac{\partial^2\phi_1}{\partial\xi^2}\right)_{|\xi=1} = \left(\frac{\partial \phi_1}{\partial \xi}\right)_{|\xi=1} - \left(\frac{\partial \phi_1}{\partial \xi}\right)_{|\xi=0}. \tag{63}$$

The right-hand side of (63) can be computed from (59) and (60) given a functional form for ϕ_1. Taylor expansion about the point $\xi = 0$,

$$\phi_1 = \xi\left(\frac{\partial \phi_1}{\partial \xi}\right)_{|\xi=0} + \tfrac{1}{2}\xi^2\left(\frac{\partial^2\phi_1}{\partial\xi^2}\right)_{|\xi=0} + \ldots, \tag{64}$$

suffices. Then substituting (64) into (60) and regrouping terms determines the linear form of (58) as

$$\frac{\mathrm{d}x_2}{\mathrm{d}t} = A - \frac{\phi_0 U_0 - BD\left[1 - (1-x_2)\dfrac{A}{B}\right]}{(1-x_2)D\left[1 - \dfrac{1-x_2}{2}\dfrac{A}{B}\right]}. \tag{65}$$

Integration implicitly yields $x_2(t)$ through

$$t = \frac{B}{A_2}\ln\left[\frac{(1-x_2)^2 + E^2}{E^2}\right] + \frac{E}{A}\arctan\left[\frac{1-x_2}{E}\right] - \frac{1-x_2}{A}, \tag{66}$$

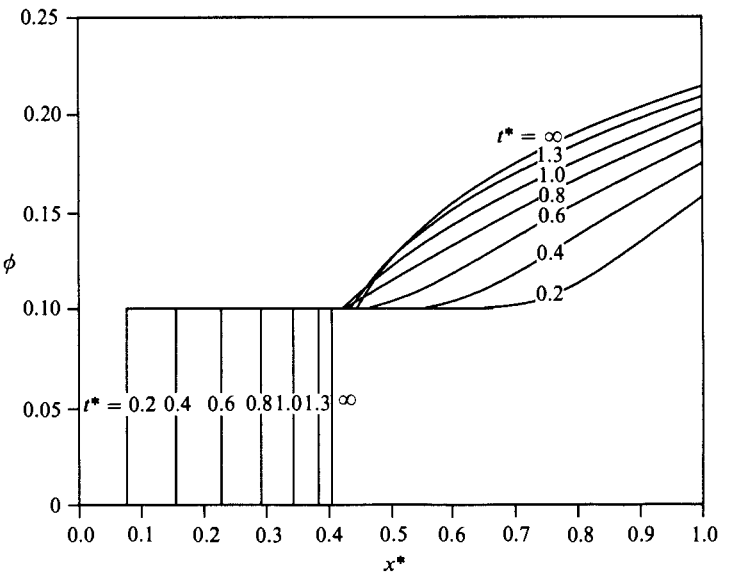

FIGURE 8. Concentration profiles at various time for flocculated dispersion for $n = 4$, $\phi_0 = 0.1$ and $Pe = 0.05$.

where A, B, D, E are constants defined as

$$A = \frac{\partial \phi U}{\partial \phi}(\phi_0) \tag{67}$$

$$B = \frac{U_0 \sigma_0'}{(\rho - \rho_f) g L} \tag{68}$$

$$D = \frac{\sigma(\phi_0)}{\sigma'(\phi_0)} \tag{69}$$

$$E = \left(\frac{2B(\phi_0 U_0 - BD)}{A^2 D}\right)^{\frac{1}{2}}. \tag{70}$$

The general procedure for integrating numerically (49), (50) and (51), with the boundary conditions (52) and (53), is to choose a small, but finite time t and use equations (61), (66) and (64) to provide the initial conditions for x_1, x_2, and an initial profile of concentration ϕ_1.

In order to study the influence of the interparticle force, we vary the Péclet number,

$$Pe = \frac{(\rho - \rho_f) g L}{\sigma_0}, \tag{71}$$

which represents the ratio of gravity to the magnitude of the stress. Increasing Pe, for example by centrifuging to increase the effective value of g, should produce greater compaction and therefore a higher volume fraction of solids in the sediment.

Figure 8 shows concentration profiles at successively increasing values of the time, for $\phi_0 = 0.1$, $Pe = 0.05$ and $n = 4$. At this low Péclet number ϕ remains considerably smaller at the bottom than ϕ_m, indicating significant interparticle forces throughout the column. However the upper surface of the suspension is perfectly sharp and

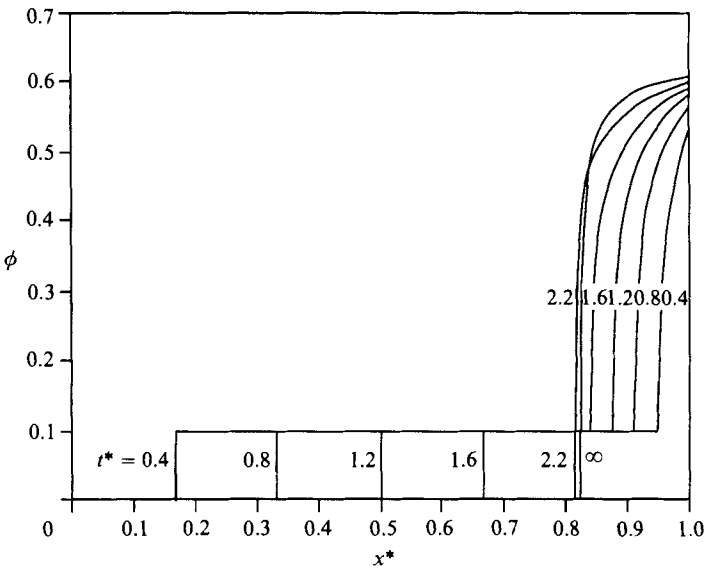

FIGURE 9. Concentration profiles at various time for flocculated dispersion for $n = 4$, $\phi_0 = 0.1$ and $Pe = 50$.

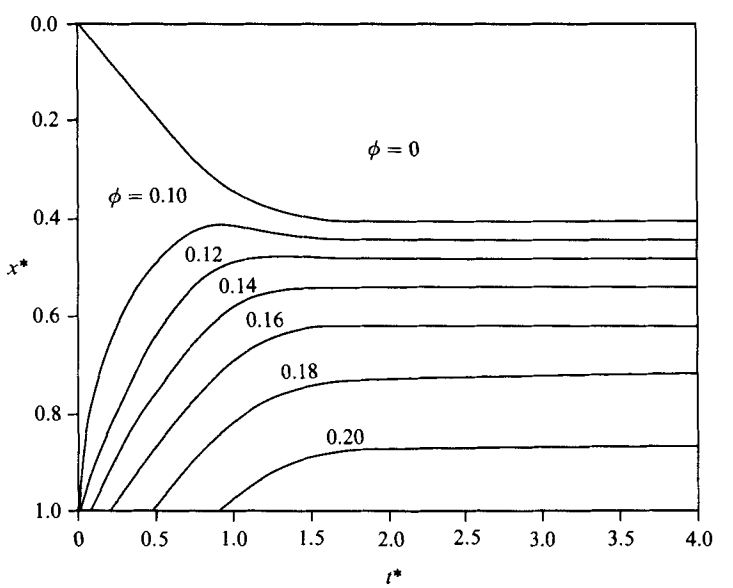

FIGURE 10. Settling behaviour showing lines of constant density for $Pe = 0.05$ for flocculated dispersion.

descends at an initially constant rate. When the network becomes strong enough to oppose further compression, a uniform zone, which has not yielded, remains. The contrast between this and a stable suspension at $Pe = 85$, which shows a diffuse upper boundary and no discontinuity in $\mathrm{d}\phi/\mathrm{d}x$, arises from the form of the stress (equation (38)) and the elastic limit of the suspension. As Pe increases to 50 (figure 9), the sediment builds up with a much sharper surface, but does not yet reach

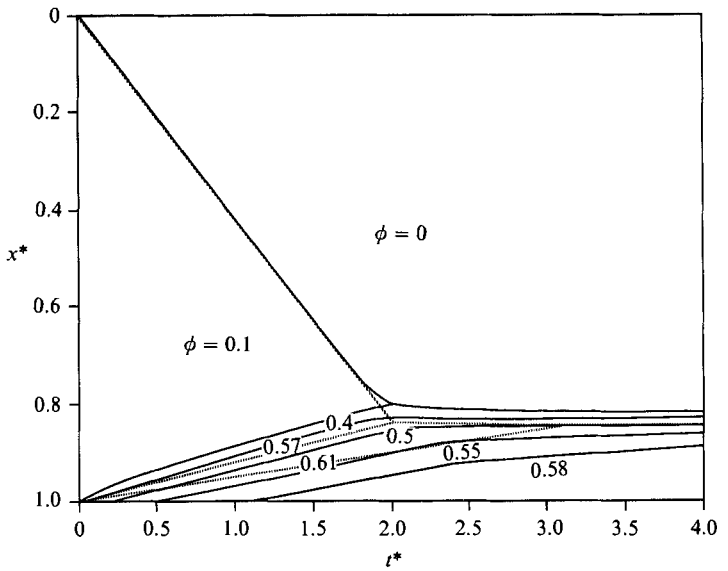

FIGURE 11. Settling behaviour showing lines of constant density for $Pe = 50$ for flocculated dispersion. $Pe \to \infty$ (Kynch case) in dashed lines.

maximum packing, indicating persistent interparticle forces transmitted throughout the suspension.

Figures 10 and 11 represent curves of constant ϕ in the (x, t)-plane for the Péclet numbers studied previously. In both cases the system reaches equilibrium at $t \leqslant 2.5$, much faster than in the stable case. The evolution of the lines of constant density of the rising sediment indicates quite different behaviour for each Péclet number. However, the rate of fall of the upper surface follows (44) with $x_2(t) - x_1(t) \sim 1$, represented by the dashed lines in figure 11, as predicted by Buscall & White (1987).

Only qualitative results can be generated at this point since the general validity of this model for flocculated materials remains to be established. However, in this concentrated regime, flocculated suspensions settle much more slowly than do stable suspensions and increasing Pe never produces total consolidation but only a new equilibrium state with a finite zone of uniform volume fraction.

8. Discussion

In the above treatment, we have developed a phenomenological theory of the sedimentation and consolidation of concentrated suspensions. The results of importance depend on the existence of momentum balances containing inertia, drag forces, and interparticle stresses, but not on the 'controversial' details of these equations which differ among the various attempts to formulate them.

The detailed analysis focused on the effects of the interparticle stresses for particles sufficiently small for inertia to be negligible. The interparticle stresses were assumed to dominate the viscous stresses associated with the consolidation process, i.e. the lubrication stresses generated by the relative motion of the particles on the microscale. The conditions for which this is true can be assessed by comparing the form expected for the viscous stress, $\mu_s \nabla \cdot \boldsymbol{v}$ with μ_s a bulk viscosity of the suspension,

with the interparticle stress σ. Since the bulk viscosity should scale on the fluid viscosity and the continuity equation dictates that

$$\nabla \cdot \boldsymbol{v} = -\frac{1}{\phi}\frac{\mathrm{D}\phi}{\mathrm{D}t} = O\left(\frac{v_t}{L}\right), \tag{72}$$

the ratio has magnitude

$$\frac{\mu_s \nabla \cdot \boldsymbol{v}}{\sigma} \sim \frac{a^2(\rho-\rho_f)g}{L\sigma_0} = Pe\left(\frac{a}{L}\right)^2. \tag{73}$$

Although $Pe \gg 1$, the ratio of particle size to the macroscopic dimension is quite small. The assumption should be valid as long as $Pe(a/L)^2 \ll 1$ provided the bulk viscosity and the interparticle stress vary in a similar manner with volume fraction.

For a colloidally stable suspension near equilibrium a simple derivation establishes that the osmotic pressure supplies the interparticle stress σ (Batchelor 1976; Davis & Russel 1988). Hence, the stress is a thermodynamic property of the dispersion and consolidation is a reversible process. Hard spheres provide a convenient model system because theory and molecular dynamics simulations have yielded accurate expressions for the osmotic pressure from infinite dilution to random close packing for a disordered fluid phase. The sedimentation process perturbs the suspension from equilibrium by an amount proportional to the microscopic or particle Péclet number, $Pe_p = 4\pi a^4(\rho-\rho_f)g/3kT$. Thus the theory remains valid for $Pe(a/L) \ll 1$, a more stringent requirement than (73).

For flocculated suspensions our formulation of the problem assumes a space filling network of particles with a volume-fraction-dependent elastic limit, or compressive yield stress. Exceeding the yield point initiates a plastic deformation which consolidates the network irreversibly into a more concentrated state. The stress is represented by a simple expression (38), consistent with the limited experimental data available. The theory does not apply for weak flocculation, since thermal fluctuations could induce a time-dependent consolidation, or when rapid consolidation ruptures the network into discrete flocs.

In the framework of our study shocks appear under well-defined conditions as apparent discontinuities in volume fraction, i.e. thin regions of large gradients. The conditions derived for the existence of shocks provide a physical basis for the 'entropy condition' of Lax. An estimate of the thickness of the shock separating regions with volume fraction ϕ_1 and ϕ_2 can be obtained from (22) (omitting the term in $v_t^2 h(\phi)/gL$ since we have not pursued the case where inertia dominates). As $|x| \to \infty$ the solution approaches ϕ_1 or ϕ_2 asymptotically. $\partial\phi/\partial x$ approaches zero at both limits and its magnitude is largest at some intermediate point. A simple measure of the dimensionless thickness (x_2-x_1) of the shock is then given by

$$x_2-x_1 = \frac{|\phi_2-\phi_1|}{\left|\dfrac{\partial\phi}{\partial x}\right|_{\max}}. \tag{74}$$

Since the quantity in brackets on the right-hand side of (22) represents the vertical separation y between the flux curve and the chord joining points on this curve with abscissas ϕ_1 and ϕ_2, the above may be written

$$x_2-x_1 = \frac{|\phi_2-\phi_1|}{gL(\rho-\rho_f)}\left|\frac{\mathrm{d}\sigma/\mathrm{d}\phi}{y}\right|_{\max}. \tag{75}$$

In particular if the flux curve is smooth and $|\phi_2-\phi_1|$ is small, $|y|_{\max} \sim |\phi_2-\phi_1|^2$ and the variation of $\mathrm{d}\sigma/\mathrm{d}\phi$ within the interval (ϕ_1, ϕ_2) can be neglected. Thus, for 'weak' shocks (75) gives

$$x_2-x_1 \sim \frac{|\mathrm{d}\sigma/\mathrm{d}\phi|}{gL(\rho-\rho_f)\,|\phi_2-\phi_1|}. \tag{76}$$

This increases without bound as $|\phi_2-\phi_1| \to 0$, so 'weak' shocks become thick, the steady state hypothesis breaks down, and their treatment as discontinuities becomes inappropriate. However, this situation is easily handled by numerical solution of the full equations. The physical thickness $L(x_2-x_1)$ of recognizable shocks depends on the parameter

$$\frac{\mathrm{d}\sigma/\mathrm{d}\phi}{(\rho-\rho_f)g} = \frac{L}{Pe}\frac{1.85\phi_m}{(\phi_m-\phi)^2} \tag{77}$$

for a stable suspension. Thus the thickness is $O(L/Pe)$ and shocks effectively disappear for $Pe \leqslant O(1)$.

The forms chosen for $U(\phi)$ and $\sigma(\phi)$ serve to illustrate the qualitative features of the phenomena. For colloidally stable suspensions numerical solutions of the transient sedimentation equations for various Péclet numbers remove any uncertainty about the validity of the results of §4. In the limit as $Pe \to \infty$ the solutions collapse to those obtained analytically provided all chords representing discontinuities lie below the flux curve. The characteristics of the discontinuities reflect the form of the flux curve and the nature of the interparticle stresses. Within the sediment the numerical results approach the Kynch solution slowly since the osmotic pressure becomes large as $\phi \to \phi_m$. For flocculated systems with $Pe \sim O(1)$ the interparticle stresses remain important throughout the network and a discontinuity appears only at the top interface between the suspension and clear fluid. Increasing the Péclet number increases the concentration of the sediment at the bottom of the vessel and would eventually generate similar discontinuities, but at values of the Péclet number well beyond those considered. The differences between the volume fraction profiles of the stable and flocculated cases at finite Péclet numbers show the importance of the nature of the interparticle stresses.

9. Conclusion

The object of this study has been to develop a theory to predict the transient settling of stable and flocculated dispersions. Kynch's theory of sedimentation represents a limiting case of a more general treatment which includes inertial effects and interparticle forces and accounts for the presence of a compaction zone at the bottom. The examination of the relative sizes of the different dimensionless parameters determines when stresses dominate the effects of inertia. Under these conditions, when particles pass through a shock, they are decelerated by those stresses as they enter a zone of higher concentration. A graphical interpretation shows that retarding forces associated with the stress transmitted between particles determine which shocks are permissible. Numerical computations demonstrate that, even as the Péclet number goes to infinity, these stresses are still important across the shocks, but the solutions do reproduce the Kynch discontinuities in the limit.

Incorporation of a compressive stress allows us to describe the consolidation of flocculated networks. Flocculated dispersions behave differently from the stable systems and respond in a way determined by the stress which can be supported by

the network. For a stable system the sediment attains maximum packing, regardless of the size of the body force causing settling. For a flocculated system, on the other hand, the asymptotic packing density depends on the magnitude of this body force, and increases as the force increases. But we should note that the mutability and the complexity of the floc structure can affect and greatly complicate the constitutive relations for the stress σ and the uniform settling velocity U. Because flocculated networks do not show a unique type of behaviour, more data should be generated to test those relationships in detail.

Acknowledgment is made to the Donors of the Petroleum Research Fund, administered by the American Chemical Society, for the partial support of this research through PRF 18165-AC7, to the National Science Foundation for support through the Particulate and Multiphase Processes Program, and also to Westvaco Corporation for supplementary support. The authors are indebted to Dr R. Buscall for invaluable suggestions on the theory of the flocculated case.

REFERENCES

ADORJÁN, L. A. 1975 A theory of sediment compression. *11th Mineral Processing Congress, Cagliari*, pp. 297–318.

ANDERSON, T. B. & JACKSON, R. 1967 A fluid mechanical description of fluidized beds. *Ind. Engng Chem. Fundam.* **6**, 527–539.

BATCHELOR, G. K. 1972 Sedimentation in a dilute dispersion of spheres. *J. Fluid Mech.* **52**, 245–268.

BATCHELOR, G. K. 1976 Brownian diffusion of particles with hydrodynamic interactions. *J. Fluid Mech.* **74**, 1–29.

BEEN, K. & SILLS, G. C. 1981 Self weight consolidation of soft soils: an experimental and theoretical study. *Geotechnique* **31**, 519–535.

BRINKMAN, H. C. 1947 A calculation of the viscous force exerted by a flowing fluid on a dense swarm of particles. *Appl. Sci. Res.* A **1**, 27–34.

BUSCALL, R., GOODWIN, J. W., OTTEWILL, R. H. & TADROS, TH. F. 1982 The settling of particles through newtonian and non-newtonian media. *J. Colloid Interface Sci.* **85**, 78–86.

BUSCALL, R. & WHITE, L. R. 1987 The consolidation of concentrated suspensions. *J. Chem. Soc. Faraday Trans.* I **83**, 873–891.

COE, H. S. & CLEVENGER, G. H. 1916 Methods for determinating the capacities of slime-settling tanks. *Trans. AIME* **55**, 356–384.

DAVIS, K. E. & RUSSEL, W. B. 1988 An asymptotic solution to the equations of sedimentation and ultrafiltration. (In preparation).

DEKRUIF, C. G., JANSEN, J. W. & VRIJ, A. 1987 A sterically stabilized silica colloid as a model supramolecular fluid. *Physics of Complex and Supramolecular Fluids*, pp. 315–347. Wiley Interscience.

DIXON, D. C. 1977 Momentum-balance aspects of free settling theory. I: Batch thickening. *Sep. Sci.* **12**, 171–191.

FITCH, B. 1983 Kynch theory and compression zones. *AIChE J.* **29**, 940–947.

HINDMARSH, A. C. 1975 GEARB solution of ordinary differential equations having banded Jacobian. *UCID*-30059 REV 1, LLL, March.

KOS, P. & ADRIAN, D. D. 1974 Gravity thickening of water treatment plant sludges. Presented at AWWA national meeting, June, Boston.

KYNCH, G. J. 1952 A theory of sedimentation. *Trans. Faraday Soc.* **48**, 166–176.

LAX, P. D. 1973 *Hyperbolic Systems of Conservation Laws and the Mathematical Theory of Shock Waves.* SIAM Regional Conf. Series in Appl. Maths.

MCROBERTS, E. C. & NIXON, J. F. 1976 A theory of soil sedimentation. *Can. Geotech. J.* **13**, 294–310.

MICHAELS, A. S. & BOLGER, J. C. 1962 Settling rates and sediment volumes of flocculated kaolin suspensions. *Ind. Engng Chem. Fundam.* **1**, 24–33.

MURRAY, J. D. 1965 On the mathematics of fluidization. Part 1. Fundamental equations and wave propagation. *J. Fluid Mech.* **21**, 465–493.

RHEE, H. K., ARIS, R. & AMUNDSON, N. R. 1986 *First Order Partial Differential Equations, vol. I, Theory and Application of Single Equations*, pp. 350–360. Prentice-Hall.

SHIN, B. S. & DICK, R. I. 1974 Effects of permeability and compressibility of flocculent suspension on thickening. *Proc. 7th Intl Conf. Water Pollution Res.* Pergamon.

SHIRATO, M., KATO, H., KOBAYASHI, K. & SAKAZAKI, H. 1970 Analysis of settling of thick slurries due to consolidation. *J. Chem. Engng Japan* **3**, 98–104.

TERZAGHI, K. 1925 Modern concepts concerning foundation engineering. *Trans. Boston Soc. Civ. Engng* **12**, 1–43.

TILLER, F. M. 1981 Revision of Kynch sedimentation theory. *AIChE J.* **27**, 823–829.

WALLIS, G. B. 1963 *One Dimensional Two-Phase Flow*, pp. 190–201. McGraw-Hill.

WOODCOCK, L. V. 1981 Glass transition in the hard-sphere model and Kauzmann's paradox. *Ann. NY Acad. Sci.* **37**, 274–298.